REVIEW PAPER

ELECTROCHEMICAL APPLICATION OF FLUORINE CHEMISTRY*

N. WATANABE

Department of Industrial Chemistry, Kyoto University,
Kyoto 606 (Japan)

Many electrochemical studies have been made in the field of fluorine chemistry because of the high electronegativity, high reactivity and high electrode potential of fluorine. Typical examples of such studies are of fluorine evolution reactions on metal or carbon electrodes, electrochemical fluorinations of many kinds of organic and inorganic compounds and applications of fluorides as cathode materials in high energy density batteries. Electrochemical fluorination has some advantageous features, but is not always better than other fluorination processes. The lithium/fluorine battery is theoretically the best high energy density battery obtainable.

Electrochemical investigations in the field of fluorine chemistry have been made in our laboratory for more than twenty years.

The following topics have been chosen for review in the present paper.

I. Electrochemical Fluorination
II. Overpotential and Anode Effect on the Fluorine Evolution at Carbon Electrodes
III. New Batteries using Lithium and Two Kinds of Graphite Fluorides as Active Material
IV. Application of Graphite Fluoride in Electrochemistry through use of its Strongly Hydrophobic Properties

*Plenary Lecture delivered at the Seventh European Symposium on Fluorine Chemistry, Venice, September, 1980.

0022-1139/83/0000-0000/$03.00

In addition to these studies, other interesting work from our laboratory includes the electrochemical preparation of intercalation compounds containing fluorine and electrolysis in molten fluoride systems. Intercalation compounds are expected to be useful as good electronic conductors and also to provide the activity of batteries or catalysts. Electrolysis in molten fluoride systems is very important since the molten fluorides are very stable electrolytes over wide temperature ranges.

I. Electrochemical Fluorination

Extensive studies have been made on the electrochemical fluorination of organic compounds and have allowed its development as an important method for the large scale production of fluorocarbon compounds. However, there is still much to be done to allow the precise control of this process, improvement in yield of the desired fluorinated compounds and for energy efficiency.

Although little definite experimental evidence has been presented as yet, the mechanisms proposed so far can be classified by fluorinating agents as follows [1,2].

1) A loose complex of nickel(II) fluoride with fluorine [3,4]
2) Complexes of high oxidation state nickel fluorides with organic substrates [5,6]
3) Simple high oxidation state nickel fluorides [7]
4) Direct oxidation of organic substrates by electron abstraction [8]

Various electrochemical techniques and ESCA have been used to elucidate the mechanism of electrofluorination.[9,10,11]

(a) Anodic behaviour of nickel in liquid hydrogen fluoride(LHF)

Fig. 1 shows current density-potential curves obtained by sweeping the potential at a scan rate of 50 mV/sec. In the first run, a current peak due to the dissolution of nickel is observed at around 0.1 V. The current due to fluorine evolution is observed at potentials above 3 V, with a plateau at

around 4 V. Since stirring of the solution did not result in an increase in the current at the plateau, the appearance of the plateau can be explained in terms of the appreciable film growth on the nickel anode and of slow electron transfer through the film. At potentials above 4 V, the current density increased again. Scanning electron microscopy of the nickel anode surface showed that surface roughening occurred at high anode potentials. Polarization at high potentials led to an increase in the electrical conductivity of the anodic film.

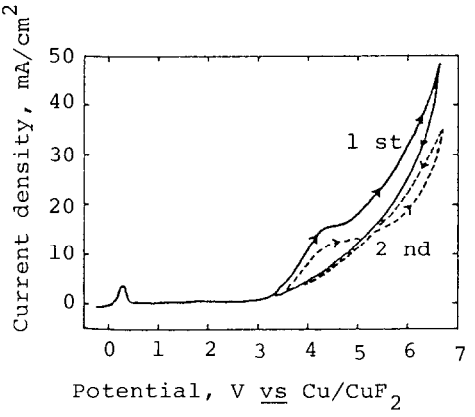

Fig.1. Polarization curves in LHF + 0.05 M H_2O.

Current-potential relations in LHF containing N-nitrosodiethylamine were nearly identical with those in LHF containing potassium fluoride. As shown in Fig. 2, the addition of N-nitrosodiethylamine to LHF did not give rise to any current peak below the fluorine evolution potential. It seemed that $Et_2N{\cdot}NO$ was fluorinated by a mechanism involving the discharge of fluoride ions or hydrogen fluoride and not by direct electron transfer from the organic compounds to the anode.

Comparison of curves A and B showed that the current for fluorination decreased with increasing concentration of $Et_2N{\cdot}NO$. This implied that $Et_2N{\cdot}NO$ was adsorbed on the anode surface and decelerated the discharge of fluoride ions.

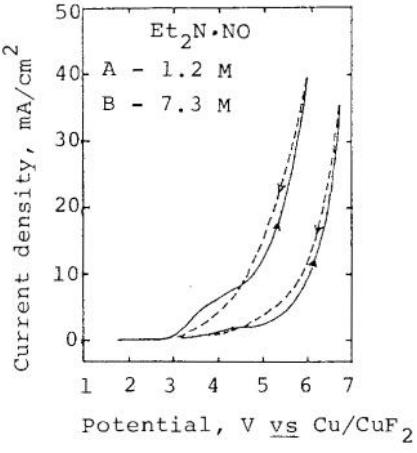

Fig.2. Polarization curves in LHF + $Et_2N \cdot NO$.

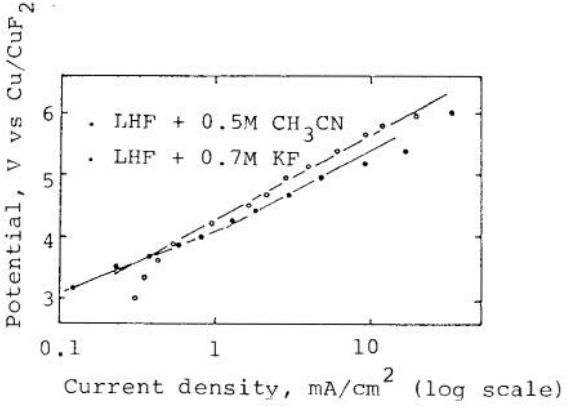

Fig.3. Steady-state polarization curves for nickel in LHF.

Fig. 3 shows typical steady-state current-potential curves for nickel in an LHF solution of KF or CH_3CN. In a KF solution, the linear relation between potential and log-[current density] had a slope of 800 mV/decade below 4 V and a slope of 1250 mV/decade above 4 V. In a CH_3CN solution, a linear relation was obtained from 4 to 6 V with a slope of 1300 mV/decade. Thus, the steady-state current for fluorine evolution and fluorination is generally represented by a Tafel-like relation.

$$E = a + b \cdot \log i \qquad (1)$$

E : anode potential

i : current density

a,b : constants

The values of b obtained in LHF were anomalously high compared with those of 60-120 mV/decade obtained for most electrode reactions in aqueous solutions [12]. Since these extremely high values seemed to be explainable by assuming that the anodic film acts as a barrier to electron transfer, the open circuit decay of anode potential was investigated to analyze the potential operating across the anodic film on nickel.

(b) Model of the electrode interface and analysis of potential decay on open circuit

A dual barrier model as shown in Fig. 4 can be assumed for the electrode reactions at a nickel anode in LHF.

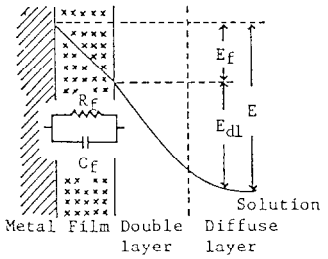

E : over-all measured potential with respect to a reference electrode

E_f : potential operating across the anodic barrier film

E_{dl} : potential across the electrical double layer

R_f : non-ohmic resistance of the film

C_f : differential capacity of the film

Fig.4 Schematic representation of the anode interface in LHF

If the electron transfer through the anodic film is the rate-determining step in the overall electrode reaction, the anodic current is represented by an exponential function of the potential operating across the film, E_f.

$$i = k \cdot c_e \exp(\alpha n F E_f / RT) \quad (2)$$

i : current across the anodic film
c_e : concentration of electron
k : rate constant of electron transfer
α : constant analogous to the transfer coefficient
n : charge number, 1

The model of the anode interface gives rise to the equation.

$$i_{ext} - i = dQ/dt = C_f \cdot dE_f/dt \quad (3)$$

i_{ext} : external measured current
Q : charge in the film
t : time

On opening the electrical circuit, $i_{ext} = 0$, and substitution of eqn.(2) into (3) and integration yields.

$$E_{f \cdot t} = E_f + b \cdot \log\theta - b \cdot \log(t + \theta) \quad (4)$$

$E_{f \cdot t}$: potential across the film at decay time of t sec.

$$b : 2.3\ RT/\alpha nF \quad (5)$$

$$\theta : (b \cdot C_f / 2.3\ k \cdot c_e) \exp(\alpha n F E_f / RT) \quad (6)$$

Eqn.(4) is depicted in Fig. 5, where $E_{f \cdot t}$ is plotted against log t and log(t + θ). The plot of $E_{f \cdot t}$ vs log(t + θ) yields a straight line with a slope of -b. When t is much larger than θ, $E_{f \cdot t}$ becomes a linear function of log t. Since the potential decay was observed over a long time in the present investigation, the values of b and θ were determined by a linear extrapolation of a $E_{f \cdot t}$ vs log t plot.

The differential capacity of the anodic barrier film can be calculated by using equation (7) obtained from equations (2) and (6).

$$b \cdot C_f = 2.3\ \theta \cdot i \quad (7)$$

The non-ohmic resistance of the film, R_f, to which the reciprocal of $k \cdot c_e$ corresponds, can be estimated by using equation (8) obtained by substituting $E_{f \cdot t} = 0$ into equation (4)

$$t^* = b \cdot C_f / 2.3(1/k \cdot c_e - 1/i) \quad (8)$$

t^* : time required for the complete decay of the potential across the film

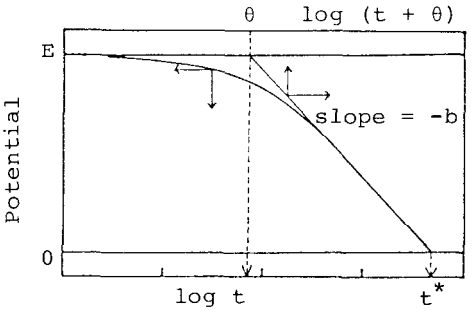

Fig. 5. Theoretical potential decay curve on open circuit.

Potential decay measurements were made on the nickel electrodes polarized at various potentials and the electrical properties of the anodic film were evaluated using the above equations. A detailed discussion of the change of the electrical properties of the film was reported previously [9,13].

Typical potential decay curves are shown in Fig. 6. In anhydrous LHF, the potential decayed logarithmically with time up to 1 sec and was arrested at around 2.5 V, the approximate fluorine evolution potential. The initial open circuit potential, about -0.2 V, was reached in about 1000 sec. The decay of potential up to 2.5 V corresponds to the potential operating across the film, E_f, since its slope was nearly identical with that of steady-state current-potential curve and it was arrested at around the fluorine evolution potential.

The time and potential at the potential arrest are regarded as t^* and E_{dl}, respectively. The slow potential decay from E_{dl} to the initial open circuit potential might be due to the diffusion of fluorine absorbed in the film into the solution. In LHF containing 0.56 M water, the decay of potential from E_{dl} was over in 100 sec, one order of magnitude shorter than in anhydrous LHF. It is probable that the absorbed fluorine was removed by the reaction with water. In LHF containing $Et_2N{\cdot}NO$, the time to reach the initial open circuit potential was longer than in LHF containing water, but shorter than in anhydrous LHF. Therefore, it seems likely that absorbed fluorine acts as a fluorinating agent.

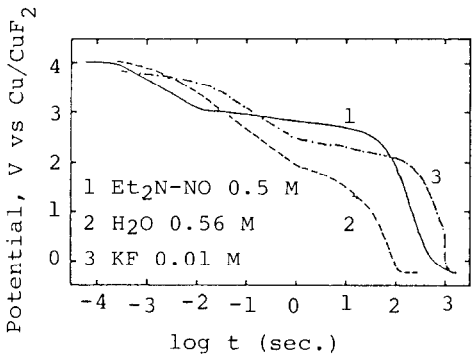

Fig.6. Potential decay curves for nickel in LHF.

(c) Growth of the anodic film on nickel and absorption of fluorine

Fig. 7 shows a cathodic stripping curve for nickel anodized at 5.2 V in anhydrous LHF for 10 minutes. Cathodic current with only one peak was observed at potentials below 2.6 V, the current began to increase rapidly at -1.0 V owing to hydrogen evolution. The reduction coulombs calculated from the area inside the curve can be assigned to the amount of fluorine absorbed in the anodic film, since the reduction curve showed that the only species being reduced was fluorine.

When the reduction coulombs thus obtained are plotted against the logarithm of the anodization time, a linear relation is obtained. If it can be assumed that the amount of fluorine absorbed in the film is proportional to the film thickness, d, the rate expression for the growth of the film is represented by equation (9).

$$d/d^\circ = \log t + \text{const.} \tag{9}$$

d° : initial film thickness

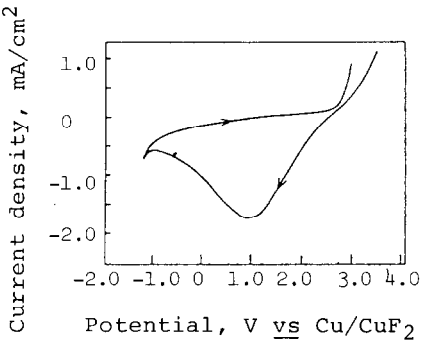

Fig.7. Cathodic stripping curve for Ni polarized at 5.2 V in anhydrous LHF; scan rate, 50 mV/sec.

As approximately linear relations were observed for log-log plots of current density vs time at potentials below 4 V, the potentiostatic i-t relation would be represented by equation (10).

$$\log i = r - s \cdot \log t \tag{10}$$

r,s : constants

The linear relation means that the surface oxide film acts as a barrier to charge transfer [14,15]. If electron transfer through the film is assumed to occur by a quantum-mechanical tunnel effect and to be rate-determining, the relationship between current and film thickness d is [16-18]

$$\log i = \log k \cdot c_e + (nFE_f/2.3\ RT) - d/d^\circ \tag{11}$$

where d° is a constant dependent on the applied potential.

Equation (11) seemed to be valid for fluorine evolution and fluorination since substitution of equation (9) for d in equation (11) gave a linear relation between log i and log t as expressed by equation (10).

(d) ESCA study of the anodic film on nickel electrodes

Since most anodic films are thin and amorphous, X-ray or electron diffraction methods cannot be effectively applied to their study. However, ESCA has a high surface sensitivity to fractions of the monolayer films and can provide elemental analysis. An ESCA study was therefore made of the anodic films formed on nickel at various potentials in LHF and LHF solutions containing water and organic compounds [19,20].

The anodic film in liquid hydrogen fluoride consisted of fluorides of nickel even at very low water concentrations. The composition of the films changed characteristically over the film depending on the amount of water contained in the LHF. The atomic ratio of fluorine to oxygen was highest at the surface region of the anode in solutions containing less than 5×10^{-3} M of H_2O whereas the addition of 0.5 M H_2O rendered it lowest at the surface region throughout the film and reduced the film thickness. The F_{1s} spectrum of nickel polarised at 6.5 V in a solution containing less than 5×10^{-3} M of H_2O indicating that fluorine was dissociatively absorbed in the film and therefore that this species might act as a fluorinating agent for perfluorination of organic compounds in liquid hydrogen fluoride.

(e) Discussion

Our results of various electrochemical measurements using nickel anodes in LHF and LHF solutions containing organic compounds, ESCA studies on the anodic film, and electrofluorination of acetonitrile support mechanism(1) i.e. a weak complex of Ni(II) fluoride and fluorine as fluorinating agent. The results of open-circuit potential decay measurements, cathodic stripping measurement, and ESCA studies of the anodic film on nickel indicate that dissociatively absorbed fluorine in the anodic film on nickel acts as an fluorinating agent and that the formation of this fluorinating agent is the rate-determining step in the over-all fluorination reaction.

The mechanism of fluorination of organic compounds by the absorbed fluorine has been discussed in the electrofluorination of acetonitrile [13]. Noteworthy differences in the fluorination of acetonitrile were observed between the electrochemical and chemical methods. We have shown that the fluorination by fluorine gas yielded fluorocarbons, CF_2 = NF, $C_2F_5NF_2$, and polymers containing nitrogen, and that no compound retaining a nitrile group was obtained [21]. Further, the amount of partially fluorinated ethanes and methanes was much larger than that of perfluorocarbons. Therefore, it is supposed that the addition of fluorine to the nitrile group takes place before the replacement of hydrogen in the methyl group by fluorine.

According to Nerdel [22], fluorination of acetonitrile by HgF_2 yielded CH_3CF = NF, $CH_3CF_2NF_2$, CH_2 = $CFNF_2$. Only addition of fluorine to a nitrile group took place and the replacement of hydrogen by fluorine was very small. These results are reasonable in view of the greater ease of addition to CH_3CN as compared with substitution.

In contrast to the above chemical methods, the electrochemical method was capable of yielding CF_3CN in a yield of more than 50%. The molar yield of CF_3CN increased appreciably with increasing rate of flow of helium flush gas, whereas those of C_2F_6 and NF_3 decreased. It should also be noted that in the electrochemical method the only fluorocarbons retaining hydrogen were C_2F_5H and a trace of CF_3H, of which the molar formation ratios were less than 10% in total.

These features indicated that, contrary to the sequence of reactions using chemical methods, the replacement of hydrogen in the methyl group took place before addition of fluorine to the nitrile group. This selectivity of fluorination suggests that fluorination by the absorbed fluorine is a two dimensional reaction which occurs on the electrode surface.

Since hydrogen fluoride is a relatively strong acid, nitrile groups in LHF are protonated and solvated by hydrogen fluoride [23]. This is shown by the abrupt increase of the electrical conductivity of anhydrous LHF on addition of a small amount of acetonitrile. Thus, acetonitrile is likely to be adsorbed on the anodic film with its methyl group oriented to the electrode and its nitrile group pointing towards the solution. This may allow preferential attack of the absorbed fluorine on the methyl groups. If fluorination occurs through the formation of complexes of high-oxidation state nickel fluorides with organic substrates, it would be difficult to explain the selectivity of fluorination in the electrochemical fluorination.

II. Overpotential and Anode Effects on Fluorine Evolution at Carbon Electrodes

The anodic overpotential for fluorine evolution on a carbon electrode in the molten salt KF·2HF is much higher than that of other anode reactions [24]. A large anode effect often occurs even at as a low current density as 0.2 A/cm^2. This is characterized by a sudden decrease in current accompanied by an increase in cell voltage and arc discharge.

There are two kinds of overpotential in the fluorine evolution reaction on a carbon anode. One is called a 'quick overpotential (π_q)" which is the rate-determining step in the discharge of fluoride ion on the carbon surface [25]. The value of π_q is about 500 millivolts. The other is called a 'slow overpotential (π_s)" which increases with the lapse of time, and in the extreme case is called the 'anode effect'. This overpotential is dependent on the inert surface of a carbon electrode. In our early studies, we thought that parts of the electrode surface are changed to a graphite fluoride during the fluorine evolution reaction and the changed portion is inactive in the anode reaction because the graphite fluoride is a very low surface-energy compound. However, the graphite fluorides are decomposed by thermal reactions and the electrode surface can return to an active surface again.

The carbon anode reaction in a fluoride cell is considered to consist of three simple processes:

1) fluorine evolution,

$$2F^- \longrightarrow F_2 + 2e \tag{12}$$

2) electrochemical formation of graphite floride from fluoride ion (F^-) and carbon (C),

$$F^- + C \xrightarrow{k_1} \text{graphite fluoride} + e \tag{13}$$

3) thermal decomposition of graphite fluoride,

$$\text{graphite fluoride} \xrightarrow{k_2} C + CF_4 \tag{14}$$

On the assumption of Langmuir-type adsorption and a linear relationship of current and voltage, the rate of the formation of graphite fluoride (v_1) on the carbon anode can be expressed as a function of potential, f(V),

$$v_1 = k_1(1-\theta)f(V) \tag{15}$$

where k_1 is the rate constant for reaction (13) and θ is the amount of surface covered by graphite fluoride. On the assumption of a first order decomposition reaction, the rate of decomposition v_2 for equation (14) is independent of the anode reaction (12) or (13).

$$v_2 = k_2\theta \tag{16}$$

Therefore, the rate of surface coverage by graphite fluoride, $d\theta/dt$, is given by equation (17).

$$d\theta/dt = k_1(1-\theta)f(V) - k_2\theta \tag{17}$$

Numerical treatment of equation (17) under the Tafel I-V relationship and Langmuir-type adsorption conditions by the potentiodynamic method was sketched in a chloride melt [26] and gave solutions as follows:

$$Kd\theta/dt = k_1(1-\theta)\exp\{(V-V_1)/b\} - k_2\theta \tag{18}$$

$$I = k_0(1-\theta)\exp\{(V-V_0)/b\} \tag{19}$$

where K is the charge required to form a non-wetting film (coul./cm^2), V, V_1 and V_0 (volts) are the anode potential and

the equilibrium potentials of reactions (13) and (12), respectively, I is current density (A/cm^2), k_0 is the exchange current density of reaction (12), θ is the surface coverage by graphite fluoride film, and b is Tafel's b coefficient. If the first term of the right-hand side of equation (17) is nearly zero or it is smaller than k_2, no anode effect occurs.

As the constants, k_1, k_2, and b, etc. depend on the crystallinity of carbon electrode, the operation or bath temperature and the kind of electrolyte, a numerical study of the anode effect using a fluoride melt is more complicated than that in the chloride melt. The formation [27] and decomposition [28] reactions by equations (2) and (3) were studied experimentally. The tendency for occurrence of the anode effect is most generally indicated by the critical current density (CCD) and its physical meaning has been discussed in detail [29]. The most important factors affecting the critical current density are the degree of graphitization of the carbon anode and existence of colloidal materials in the bath [30].

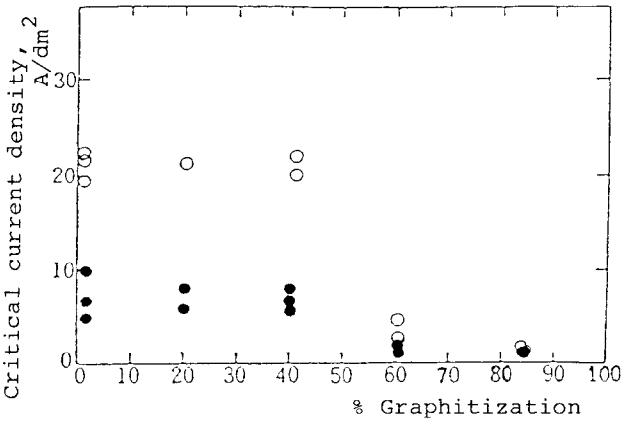

Fig.8. Effect of degree graphitization on critical current density.
● : NiF_2 addition, ○ : no addition

Fig. 8 shows the relation between the degree of graphitization of the anode and the CCD at which the anode effect occurs. The anode effect occurs more often on a carbon anode graphitized more than 50%, whether colloidal particles of NiF_2 are absent or present. The effect of a fluoride on the anode effect was also observed with many other sparingly soluble fluorides such as AlF_3, CaF_2 incorporated into the bath. The most successful result was obtained with LiF which is slightly soluble (about 0.8 wt%) in the fluoride bath (KF-2HF) at 100°C. The relationship between the CCD and amount of LiF added to the bath is shown in Fig. 9.

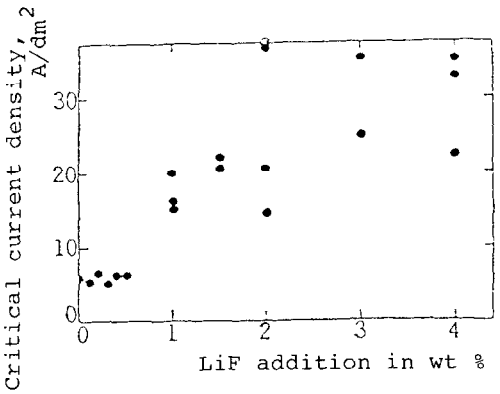

Fig.9. Effect on LiF addition on critical current density.

The effect of LiF addition on the CCD was more than solubility would indicate,as seen from the Figure. The mechanism of the addition effect has not yet been elucidated; however, we have made the following suggestion:

1) The neutralization of fluorine gas bubbles by colloidal particles [31].

As the fluorine gas bubbles have negative charges and are strongly attracted to the anode, the charged bubbles may be neutralized by absorption of positively charged colloidal particles. However, an experiment designed to determine the zeta-potential of the gas bubbles and the colloidal particles was a failure [32].

2) Mechanical removal of the thin film of graphite fluoride by the colloidal particles.

3) Formation of an intercalation compound film, e.g. CF_xLiF, on the carbon surface.

Various intercalation compounds are formed by the reaction of solids such as LiF, MgF_2, AlF_3, and graphite in the presence of fluorine at room temperature. These compounds are of higher surface energy than graphite fluorides.

The third proposal seems most likely from the experimental results. However, the anode effect still leaves some unanswered questions. For example, what kind of graphite fluoride film is formed on the anode surface and how much surface coverage by the film is necessary for the occurrence of an anode effect?

III. New Batteries using Lithium and Two Kinds of Graphite Fluorides as Active Materials

A battery based on a lithium-fluorine system is ideal from their positions in the periodic table, but it is not easy to use elemental fluorine as the cathode active mass. 17 Years ago, we were surprised to find that the surface of a glass sample bottle in which a graphite fluoride was stored for a long time became tarnished, because graphite fluoride should be a very stable and non-reactive material [33]. From this observation, it was postulated that fluorine was absorbed in active carbon at room temperature. The carbon with absorbed fluorine (C...F) has a high electrical conductivity and does not liberate fluorine gas by heating. On heating the fluorine becomes chemically bonded to carbon and the solid changes to a graphite fluoride as equation (20). And the (C...F) oxidizes iodide to iodine as equation (21).

$$nC + \frac{n}{2} F_2 \xrightarrow[\text{temp.}]{\text{room}} n(C...F) \xrightarrow{\text{heat}} (CF)_n \qquad (20)$$

$$2(C...F) + 2KI \longrightarrow I_2 + 2KF \qquad (21)$$

These findings led us to our new high energy battery containing a combined system of lithium and graphite fluoride, and Matsushita Electric Company have developed a commercially available lithium battery. In Matsushita's batteries, a graphite fluoride is now used instead of (C...F) as the cathode material, because (C...F) electrode facilitates discharge itself.

Fig. 10 shows the relationship between open circuit voltage (OCV) and discharge percentage of the battery for a system of lithium and $(CF)_n$ or $(C_2F)_n$ electrodes at 30°C in 1M $LiClO_4$-propylene carbonate (PC) solution [34]. The average initial OCV's were 3.20 and 3.22 V, and the discharge currents were kept constant at 2 mA/cm^2. The open circuit voltages were measured every two hours after termination of the polarization. They decreased rapidly after the initial discharge and, thereafter, became virtually constant at around 3.0 V versus Li for the $(C_2F)_n$ electrode and around 2.8 V versus Li for $(CF)_n$. The OCV after completion of the discharge was 2.4 V vs Li for both electrodes.

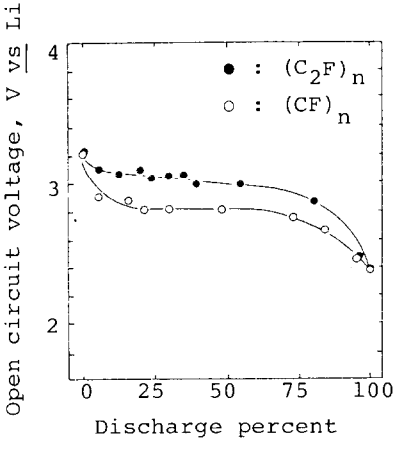

Fig.10. Change of open circuit potential of $(CF)_n$ and $(C_2F)_n$ electrodes with percentage discharge in 1 M $LiClO_4$-PC at 30°C.

The relationships between discharge voltages and time at a constant current density (0.5 mA/cm^2) are shown in Fig. 11. The distinctive features for both batteries are high energy density, high voltage and stable discharge potential. In particular, the discharge potential and efficiency of utilization of the battery using $(C_2F)_n$ are higher than those of the battery using $(CF)_n$. However, if the cell reaction is postulated to be equation (22),

$$(CF)_n + nLi \longrightarrow nLiF + nC \qquad (22)$$

the OCV must become 4.6 V from the thermodynamic properties of lithium fluoride and graphite fluoride [35]. The discrepancy is because of formation of a ternary intercalation compound by the initial cell reaction:

$$(CF)_n + nLi + mPC \longrightarrow C_n(LiF)_n \cdot mPC \ (^{\text{electrochemical}}_{\text{reaction}}) \qquad (23)$$

followed by

$$C_n(LiF)_n \cdot mPC \longrightarrow nC + nLiF + mPC \ (^{\text{chemical}}_{\text{reaction}}) \qquad (24)$$

where PC represents propylene carbonate, or $\overline{OCH(CH_3)CH_2OCO}$. The rate of process (24) would be slower than the initial electrochemical reaction.

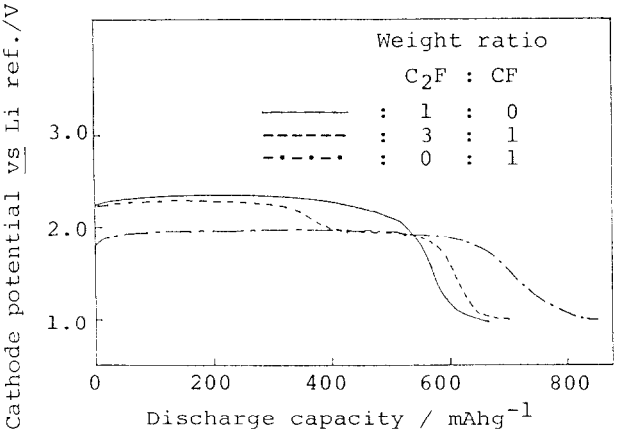

Fig.11. Discharge characteristics of mixtures of CF and C_2F (0.5mA/cm^2).

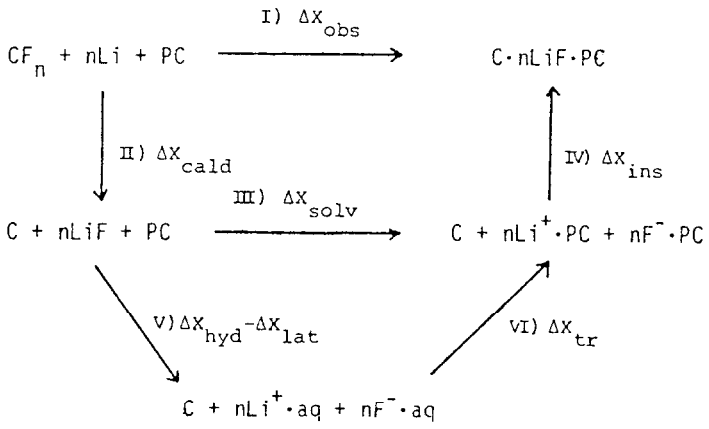

Fig.12. A relation among six processes of cell reaction.

These processes (22) to (24) are related to each other as shown in Fig. 12, where ΔX represents thermodynamic functions (X = G,H and S) and suffixes are obs : observed value, solv : solvation, calc : calculated value, ins : insertion of a solvated ion into a layered lattice of graphite, lat : lattice, tr : transfer from water to PC, and hyd : hydration. Each thermodynamic quantity for ΔX in Fig. 12 was evaluated by calculation from experimental results and various data [36]. The changes of both Gibbs free energy and enthalpy for the solvation of LiF and insertion of solvated ions while the entropy change is negative, and the increase in the free energy change corresponds to the decrease of the cell voltage. About 3.3 V in the original OCV corresponds to the formation of the ternary intercalation compound by equation (23). As the discharge reaction proceeds, the graphite intercalation compound $C(LiF)_n \cdot mPC$ formed by the electrochemical reaction gradually decomposes to graphite, LiF and propylene carbonate as shown in equation (24).

Fig. 13 shows X-ray diffraction patterns of the product immediately after careful discharge and of those heated to 300°C and to 500°C. The non-heated discharge product showed no distinct diffraction peak but a broad peak at 20 to 30° (2θ).

This implies the presence of solvent within the sample and it is said that during the discharge reaction there is an increase in thickness of the layers of $(CF)_n$. It is therefore suggested that Li^+ ions are inserted between the layers accompanied by solvent molecules. The sample heated up to about 300°C decreased in weight by 32% and showed clear peaks for solid LiF and carbon. A further sample heated to over 500°C showed an increased peak height for LiF with the peak for carbon shifted to a slightly higher angle and sharpened. The two small peaks around 30° were due to lithium carbonate formed by the decomposition reaction of PC [37] or contamination by air. The IR spectrum of the gaseous product obtained by heating to 300°C indicated that PC was released from the sample.

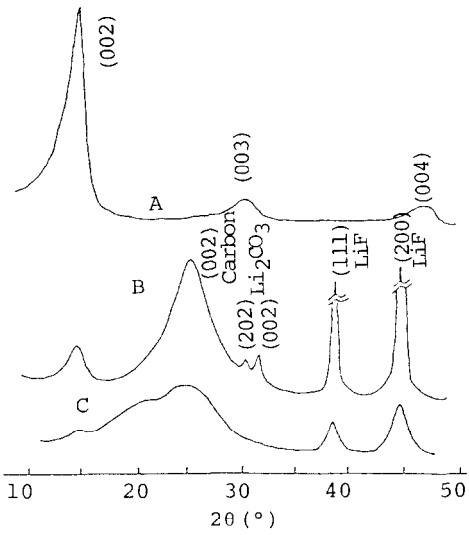

Fig.13. X-ray diffraction patterns of $(CF)_n$ and 90% discharged product with 0.5 mA in 1M $LiClO_4$-PC at 298 K. A : $(CF)_n$, B : discharge product evacuated 2 days, C : discharge product with PC.

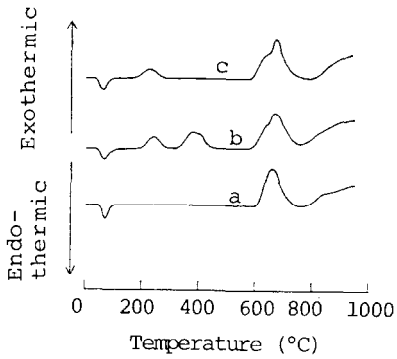

Fig.14. DTA curves for $(CF)_n$ and $(C_2F)_n$ electrodes after discharge.

a : $(CF)_n$ before discharge

b : $(CF)_n$ after discharge

c : $(C_2F)_n$ after discharge

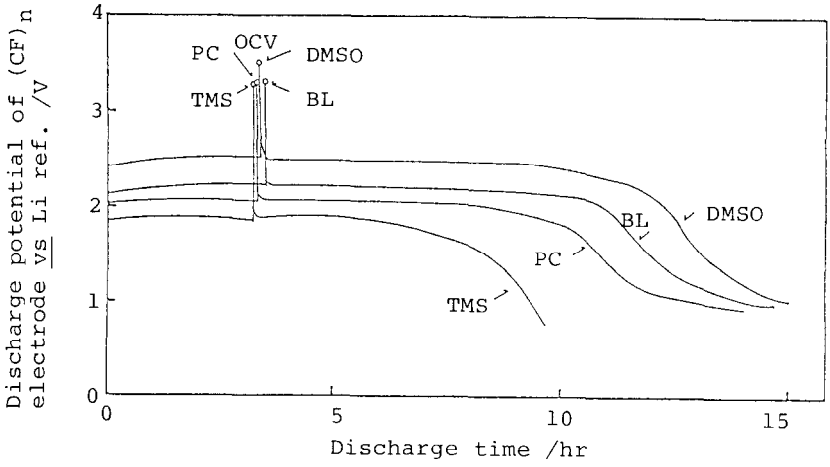

Fig.15. Discharge characteristics of $(CF)_n$ cathode in different solvents ($0.5mA/cm^2$).

DTA curves for the discharged graphite fluoride gave a broad endothermic peak around 200°C as shown in Fig. 14, near by the boiling point of PC. Moreover, the results of F_{1s}, C_{1s} and Li_{1s} photoelectron spectra of the discharge products of graphite fluorides support the formation of the intercalation compounds [33]. Therefore, the OCV and the discharge voltage of $(CF)_n$ electrode are different from the electrolytic solution as shown in Fig. 15 [38] and those of $(C_2F)_n$ electrode are similar.

IV. Application of Graphite Fluoride in Electrochemistry through Use of Its Strongly Hydrophobic Properties

Typical properties of a graphite fluoride are a low surface energy, lamellar structure, oxidizing activity and great chemical stability. These characteristics can be advantageously applied in, for example, the battery, solid lubricant and water proofing treatment industries.

One of the most important factors controlling the performance of a carbon-oxygen electrode in an alkaline solution is likely to be the wetting of porous parts of the carbon electrode by the electrolyte solution. In order to impart hydrophobicity, the carbon electrode pores have been usually coated with paraffin, polyethylene, polystyrene or polytetrafluoroethylene. Their water-proofing ability, however, is gradually reduced by electrochemical corrosion (formation of hydroperoxide) in the concentrated alkaline solution. Graphite fluoride is a unique compound which has an extremely low surface energy and great resistance to oxidation.

A porous carbon electrode was fabricated by mixing 70 wt% of an active carbon which had been prepared by the heat treatment of charcoal in an ammonia atmosphere and 30 wt% of graphite fluoride [39].

Fig. 16 shows the continuous discharge characteristics of carbon and mixed carbon-graphite fluoride electrodes in a 30% KOH solution at 25°C. The potential of the mixed electrode remained at a constant value for a long time when used as an oxygen electrode. Graphite fluoride itself does not function in the electrochemical reduction of oxygen.

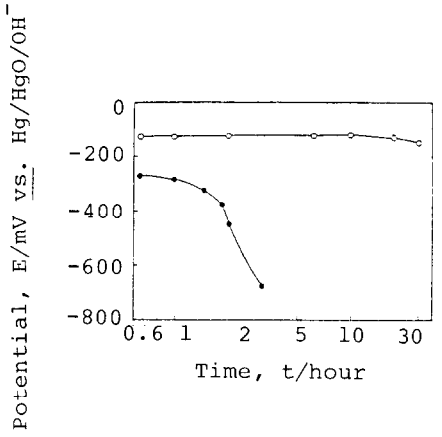

Fig.16. Continuous discharge characteristics of O_2-activated carbon electrodes.

○ : Carbon+30%$(CF)_n$ ● : Carbon
Current density : 50 mA/g

The effect is due to extremely low surface energy and high chemical stability of graphite fluoride. While less than 30 wt% of mixed graphite fluoride retains many active sites on the carbon electrode, the wetting by the electrolyte in the wick of the electrode increases appreciably over 10%. But, while more than 30 wt% of the mixed graphite fluoride is able to prevent wetting, the active sites decrease and the electrical resistance of the electrode increases. When the surface of a porous carbon electrode is coated by direct fluorination in a fluorine atmosphere at around 300°C, the electrode gives the same result [40] as above.

There is a further application for the hydrophobic properties of graphite fluorides [41]. As organic compounds are generally readily soluble in organic solvents, but only sparingly soluble in water, electrochemical preparative processes are difficult because of the low conductivity of the organic solution. Tari and Hirai [41] have achieved better results by using a hydrophobic electrode. The

graphite fluoride surface is water repellent, but is wet by an acrylonitrile solution. Therefore, the following electrode reaction proceeds at a low cell voltage because the ionic conductivity depends mainly on the strong electrolyte of aqueous solution.

$$2CH_2 = CHCN + 2H^+ + 2e^- \longrightarrow NC(CH_2)_4CN \qquad (24)$$

There are many other applications which use the low surface energy characteristics of graphite fluorides. They can be used, for example, as surface lubricants, reserve soil, etc.

ACKNOWLEDGEMENTS

The author would like to express his sincere thanks to Professor G. Gambaretto, University of Padua for inviting him to the 7th European Symposium on Fluorine Chemistry and to Professor D. W. A. Sharp, University of Glasgow for reading the manuscript and for giving many suggestions.

REFERENCES

1 J. Burdon and J. C. Tatlow, in Advances in Fluorine Chemistry, edited by M. Stacey, J. C. Tatlow and A. G. Sharpe, Vol. 1, pp. 129-165, Butterworths, 1960.
2 N. Watanabe and M. Haruta, in Fluorine Chemisty and Industry, edited by N. Watanabe, Vol. 2, pp. 131-148, Kagakukogyosha, 1973.
3 L. G. Spears and N. Hackerman, J. Electrochem. Soc., 115, 452 (1968).
4 Ch. Comninellis, Ph. Javet and E. Platter, J. Appl. Electrochem., 4, 289 (1974).
5 J. A. Donehue, A. Zlets and R. J. Flannery, J. Electrochem. Soc., 115, 1042 (1968).
6 L. Stein, J. M. Neil and G. R. Alms, Inorg. Chem., 8, 2472 (1969).
7 Ya. N. Voitovich and V. Ya. Kazakov, Zh. Priki. Khim., 44, 2452 (1971).

8 J. Burdon, 6th Int. Symposium on Fluorine Chemistry, Program and Abstract A. 13, Durham, England, July, 1971.
9 N. Watanabe, S. Matsui and M. Haruta, Denki Kagaku (J. Electrochem. Soc. Japan), 43, 638 (1975).
10 P. B. Burrows and R. Jashinski, J. Electrochem. Soc., 115, 348 (1968).
11 B. B. Damaskin, in The Principles of Current Methods for the Study of Electrochemical Reactions, pp 3, 26, 32, McGraw-Hill, 1967.
12 For example, E. Gileadi and B. E. Conway, in Modern Aspects of Electrochemistry, edited by J. O'M. Bockris, Chap. 5, pp 362.
13 M. Haruta and N. Watanabe, J. Fluorine Chemistry, 7, 159 (1976).
14 J. W. Schultze, Z. Phys. Chem., 73, 29 (1970).
15 A. Damjanovic, A. T. Ward and M. O'Jea, J. Electrochem. Soc., 121, 1186 (1974).
16 J. W. Schultze and K. J. Vetter, Electrochim. Acta, 18, 889 (1973).
17 K. J. Vetter and J. W. Schultze, Ber. Bunsenges. Physik. Chem., 77, 945 (1973).
18 P. Kohl and J. W. Schultze, ibid, 77, 953 (1973).
19 K. Siegbahn et al., in ESCA, Atomic, Molecular and Solid State Structure Studied by Means of Electron Spectroscopy , Almqvist and Wiksells, Uppsala, 1967.
20 N. Watanabe and M. Haruta, Electrochim. Acta, 25, 461 (1980).
21 J. A. Cuculo and A. Biegelow, J. Amer. Chem. Soc., 74, 710 (1968).
22 F. Nerdel, Naturwissenschaften, 39, 209 (1952).
23 R. M. Adams and J. J. Katz, J. Molecular Spectroscopy, 1, 306 (1957).
24 N. Watanabe, M. Ishii and S. Yoshizawa, J. Electrochem. Soc. Japan, 30, 171 (1962).
25 N. Watanabe, M. Inoue and S. Yoshizawa, J. Electrochem. Soc. Japan, 31, 168 (1963).
26 Y. Kanaya and N. Watanabe, J. Electrochem. Soc. Japan, 40, 417 (1972).

27 N. Watanabe, Y. Koyama and S. Yoshizawa, ibid, 32, 17 (1964).
28 N. Watanabe, S. Koyama and H. Imoto, Bull. Chem. Soc. Jpn., 53, 2731, 3093, 3103 (1980).
29 Y. Kanaya and N. Watanabe, J. Electrochem. Soc. Jpn., 40, 417 (1972).
30 N. Watanabe, M. Ishii and S. Yoshizawa, ibid, 29, E179 (1961).
31 N. Watanabe, M. Inoue and S. Yoshizawa, ibid, 31, 113, 168 (1963).
N. Watanabe and N. Ohba, ibid, 35, 130 (1967).
32 N. Watanabe and H. Imoto, ibid, 35, 178 (1967).
33 N. Watanabe and A. Shibuya, Kogyo Kagaku Zasshi (J. Chem. Soc. Jpn.), 71, 963 (1968).
34 N. Watanabe and K. Morigaki, Denki Kagaku (Electrochem. Soc. Jpn.), 47, 169, 174 (1979).
35 J. L. Wood, A. J. Valerga, R. B. Badachhape and J. L. Margrave, Final Report Contact DAABO 7-73-C-0056 (MCOM), Rice Univ. Mar. 1974.
36 K. Ueno, N. Watanabe and T. Nakajima, J. Fluorine Chemistry, 19, 323 (1982).
37 A. N. Deyand and B. P. Sullivan, J. Electrochem. Soc., 117, 222 (1970).
38 N. Watanabe, R. Hagiwara and T. Nakajima Electrochim Acta (1982), in press.
39 Y. Horita, G. Kano and N. Watanabe, Denki Kagaku (J. Electrochem. Soc. Jpn.), 50, 334 (1982).
40 Y. Horita and N. Watanabe, ibid, 37, 848 (1969).
41 I. Tari and T. Hirai, 32nd Symposium on Colloid Chemistry at Matsuyama, p.142 (1979).